EPJ manuscript No.
(will be inserted by the editor)

Electron interference and entanglement in coupled 1D systems with noise

Fabrizio Buscemi[1], Paolo Bordone[2,3], and Andrea Bertoni[3]

[1] ARCES, Alma Mater Studiorum, Università di Bologna, Via Toffano 2/2, 40125 Bologna, Italy, e-mail: fabrizio.buscemi@unimore.it

[2] Dipartimento di Scienze Fisiche, Informatiche e Matematiche, Università di Modena e Reggio Emilia, Via Campi 213/A, 41125 Modena, Italy

[3] Centro S3, CNR-Istituto Nanoscienze, Via Campi 213/A, 41125 Modena, Italy

Received: date / Revised version: date

Abstract. We estimate the role of noise in the formation of entanglement and in the appearance of single- and two-electron interference in systems of coupled one-dimensional channels. Two cases are considered: a single-particle interferometer and a two-particle interferometer exploiting Coulomb interaction. In both of them, environmental noise yields a randomization of the carrier phases. Our results assess how the complementarity relation linking single-particle behavior to nonlocal quantities (such as entanglement and environment-induced decoherence) acts in electron interferometry. We show that in an experimental implementation of the setups examined, one- and two-electron detection probability at the output drains can be used to evaluate the decoherence and the degree of entanglement.

PACS. XX.XX.XX No PACS code given

1 Introduction

In the last decades, much attention has been devoted to semiconductor systems able to control and expose the correlated dynamics of few carriers [1,2]. In particular, the study of the electron propagation in one-dimensional (1D) structures opened interesting opportunities for device applications in quantum electronics and optoelectronics, such as the single-electron transistor [3]. Beyond the design of nanometric devices, the coherent charge transport in 1D channels is also very appealing from the basic physics perspective, as it enables to analyze quantum

features, such as coherence and interference, and to relate them to the appearance of quantum correlations [4, 5]. Furthermore, it also represents a suitable means to fully exploit the potential of the entanglement as the basic ingredient of quantum information processing.

Recent experiments showed the feasibility of electron interferometers in 1D semiconductor systems, such as quantum wires [6,7] and edge states operating in the integer quantum Hall regime [8,9]. The former, relying on the quantization of conductance in narrow constrictions within two-dimensional electron gases, have been the subject of a number of theoretical [10,11,12,13] and experimental [6,14,15,16] works aimed at investigating their potential applications as quantum logic devices. In particular, the possibility of realizing a universal set of quantum gates by means of coupled quantum wires was proven in Ref. [17], where the localization of the electron in one of the two 1D channels defines a flying qubit. Recently, quantum-wire systems have been shown to be suitable to implement complex quantum computation protocols, such as quantum teleportation and Shor's factorization algorithm [18,19].

Most of the electron devices applications using 1D channels rely on the coherent propagation of carriers. As it is universally recognized, the loss of coherence of a quantum system due to the unavoidable interaction with its environment represents the major threat to the quantumness of the system itself [20,21]. Also, the working of interferometer setups or devices implementing quantum information protocols results to be jeopardized by decoherence processes. This justifies the growing attention recently devoted to the theoretical investigation of mechanisms responsible for the loss of coherence in quantum interference setups [22,23,24,25,26,27]. In these systems, the loss of coherence, resulting in a decrease of the visibility of the interference pattern, has been attributed to the thermal averaging related to the spread of the wavelengths of the carriers contributing to the current or to other dephasing mechanisms more intrinsically related to the environment features. Specifically, most of the works adopt the phenomenological "dephasing terminal" approach where an additional artificial electron reservoir randomizes the phase of electrons [23,24]. In other schemes, the environment has been modeled as a classical noise field that leads to a fluctuation of the phase difference for the electrons crossing the interferometer devices [25,26].

In this paper, we present a theoretical approach for analyzing the effect of the electron decoherence on single-electron and two-electron quantum interference and on carrier-carrier entanglement. Specifically, two different systems are examined: a single-electron Mach-Zehnder interferometer (MZI) and a device consisting of two MZIs coupled together by the Coulomb interaction operating in a two-particle regime. We also track the effects of the noise. The two-particle interferometer has been analyzed in a recent work [4], where the *which-path* measurement on one of the two MZIs has been widely discussed by using the other one as a detector and neglecting decoherence phenomena due to coupling with the environment.

In our approach, we describe the environmental noise in terms of randomization of the phases of the charge carriers traveling along the channels. In agreement with the "classical fluctuating potential" procedure [22,25], such a process is ascribed to stochastic fluctuations affecting the potential profile of the electron waveguides responsible of phase delay of the electrons. As a result, the latter phase obeys a statistical distribution related to the intrinsic features of the noise. The quantum system is thus described by the statistical mixture of the states obtained by averaging over the carrier phases. As expected, the quantumness of the system is reduced by an increasing disorder. Such a noise model represents a valuable guideline to evaluate analytically how the electron dephasing affects interference and entanglement in mesoscopic setups exploiting electron-electron interaction. In order to validate our approach, first we apply it to a simple system, that is a one-electron MZI and then we extend it to a two-electron interferometer. We focus on the complementarity relations between single-particle properties, such as single-particle visibility, predictability, and non-local quantities, such as entanglement with the remaining part of the system [28, 29,30]. Such relations, initially introduced for pure two-qubit states [28,29] and then extended to pure multi-qubit states [30], have been validated both in quantum optics [31,32] and NMR experiments [33]. Our aim is to show that the complementarity relations hold for two-electron mixed states obtained in noisy 1D technologically relevant semiconductor channels.

The paper is organized as follows: In Sec. 2, we illustrate a single-electron interferometer, implemented by means of 1D structures, and then we analyze the effects of noise on the visibility of the fringes of the single-particle interference. In Sec. 3, we discuss the coupling via Coulomb interaction of two single-electron interferometers in absence of noise and then we study the effect of their entanglement on interference phenomena. In Sec. 4, we examine how the dephasing due to noise affects both the two-particle interference and the particle-particle entanglement in the two-electron interferometer. Finally, we present our conclusions in Sec. 5.

2 Single-particle interferometer

Here, we describe schematically an electronic version of the ubiquitous optical single-particle MZI [34] exploiting electron transport in 1D structures [12,13,17,35]. The layout of the single-particle interferometer is sketched in Fig. 1.

Specifically, we consider a system of two coupled electron channels with an electron injected from the source S and propagating along x in the upper waveguide. Within the assumption of ballistic transport with no dephasing effect, the carrier is described by a plane wave with wavevector k along the x direction, while the qubit $|0\rangle$ ($|1\rangle$) is defined through the localization of the electron in the upper (lower) channel and can be expressed in terms of the localized states of a double-well potential.

The basic elements needed to perform the single-particle quantum operations are the phase shifter and the beam

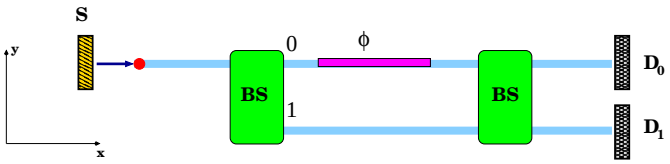

Fig. 1. Sketch of the electron MZI. A charge carrier injected from the source S reaches a beam splitter where it is split in two components: one propagating along the waveguide 0 where a potential barrier is placed, the other traveling in the waveguide 1. Both components merge at the second beam splitter, where they interfere. The particle is revealed either at the drain D_0 or at the drain D_1, e.g. by means of single-electron transistors acting as sensitive charge detectors. In the case of no decoherence effects, the phase ϕ accumulated along channel 0 is a deterministic variable. Otherwise, it is a stochastic variable described by the distribution given in Eq. (7). The electron-intensity measurements will show single particle interference depending upon the phase accumulated and upon the noise effects.

splitter. The former can be obtained by inserting a suitable potential barrier in one of the two channels, thus inducing a delay phase in the propagation of the wavefunction, as shown by a simple investigation of the electron transmission amplitude. For a particle with kinetic energy $E{=}\hbar^2k^2/2m$ and a potential barrier of height V_0 and length d, the transmission amplitude t takes the form

$$t = \frac{1}{\cos^2 k_1 d + \frac{1}{4}\left(\frac{k_1}{k}+\frac{k}{k_1}\right)^2 \sin^2(k_1 d)} \exp(i\phi), \qquad (1)$$

where $k_1{=}\sqrt{2m(E-V_0)}/\hbar$, and

$$\phi = -kd + \arctan\left[\frac{1}{2}\left(\frac{k_1}{k}+\frac{k}{k_1}\right)\tan k_1 d\right]. \qquad (2)$$

In the limit of a small barrier, i.e. $V_0 \ll E$, $|t|^2$ is close to 1, that is the electron is entirely transmitted, while the delay phase ϕ reduces to $\phi = -(kd/2)(V_0/E)$. The matrix representation of the electronic phase shifter $R_{0(1)}$ on the one-qubit basis $\{|0\rangle, |1\rangle\}$ obtained by inserting a potential in the channel 0(1) will be given by

$$R_0(\phi) = \begin{pmatrix} e^{i\phi} & 0 \\ 0 & 1 \end{pmatrix} \qquad \text{and} \qquad R_1(\phi) = \begin{pmatrix} 1 & 0 \\ 0 & e^{i\phi} \end{pmatrix}. \quad (3)$$

The electron beam splitter can be obtained by suitably tuning, in a coupling region along the propagation direction, the potential profile forming the two quantum channels [15]. Specifically, it has been shown that the carrier wavefunction in the transversal direction oscillates by lowering the potential barrier between the quantum wells defining the quantum channels in the transversal direction [13,17]. This process terminates when the carrier reaches the end of the coupling region and the electron wavefunction is separated into two components travelling along the upper and the lower channel. The matrix representation of such one-qubit transformation reads

$$R_y(\theta) = \begin{pmatrix} \cos\frac{\theta}{2} & i\sin\frac{\theta}{2} \\ i\sin\frac{\theta}{2} & \cos\frac{\theta}{2} \end{pmatrix}, \qquad (4)$$

where the phase θ depends upon the physical and geometrical parameters of the coupling region and the electron energy [36].

2.1 No decoherence

Here, we investigate the behavior of the one-particle interferometer illustrated in Fig. 1, when no source of electron

decoherence is considered. The electron arriving at the drains D_0 and D_1 is described by a pure single-particle state $|\Psi_{OUT}\rangle$. This is related to the input state $|\Psi_{INP}\rangle$=$|0\rangle$ by:

$$|\Psi_{OUT}\rangle = R_y\left(\frac{\pi}{2}\right) R_0(\phi) R_y\left(\frac{\pi}{2}\right)|\Psi_{INP}\rangle$$
$$= ie^{i\frac{\phi}{2}}\left(\sin\frac{\phi}{2}|0\rangle + \cos\frac{\phi}{2}|1\rangle\right). \qquad (5)$$

where $R_y\left(\frac{\pi}{2}\right) R_0(\phi) R_y\left(\frac{\pi}{2}\right)$ describes the network of quantum gates implementing the single-electron MZI. In the measurements performed at the output drain $D_{0(1)}$, the detector response function is proportional to the square modulus of the 0(1) wavefunction component, namely

$$|\sin\frac{\phi}{2}|^2 (|\cos\frac{\phi}{2}|^2). \qquad (6)$$

Such oscillations depending upon ϕ in the electron intensity (or in the coherent component of the current) are a manifestation of the single-particle interference. The visibility of interference patterns, given by ν=$\left(I_{\max} - I_{\min}\right) / \left(I_{\max} + I_{\min}\right)$, where $I_{\max(\min)}$ indicates the maximum (minimum) signal intensity revealed by a charge detector in the drain $D_{0(1)}$, is equal to the optimal value of 1.

2.2 Decoherence

The effects due to the loss of electronic coherence on the functioning of the single-electron MZI sketched in Fig. 1 are now examined.

In our scheme, the classical noise is described in terms of the fluctuations of the potential profile along the propagation direction of the carriers, while along y the double-well potential is assumed to be immune from noisy effects. This means that no undesired channel mixing due to environment action can occur, only those noise mechanisms leading to a randomization of the phase of the carriers are considered.

As shown above, the potential barrier inserted in channel 0 induces a delay phase linearly depending upon the width and the height of the barrier itself. In close analogy with the procedure used in Ref. [22], the potential barrier parameters are supposed to fluctuate according to a stochastic behavior as a consequence of the noise. This also implies the randomness of the delay phase ϕ. For the sake of simplicity, the latter is assumed to be described by a flat distribution

$$P(\phi) = \begin{cases} 1/\Delta\phi & \text{for} \quad |\phi - \phi_0| \leq \Delta\phi \\ 0 & \text{otherwise} \end{cases}, \qquad (7)$$

where ϕ_0 is the delay phase value in the absence of noise and $\Delta\phi$ is a measure of the decoherence effects induced by the environment, that is of the "noise intensity". In fact, when $\Delta\phi$ goes to zero the noise effect vanishes, while for $\Delta\phi = 2\pi$ the maximum dephasing is obtained. The choice of a flat probability distribution allows one to solve analytically the system, and therefore, to provide an initial guideline for the analysis of decoherence phenomena in more general cases.

In strict analogy with the random field approaches introducing classical noise in quantum system [37,38,39], the quantum state describing the electron at the output drains will be given by the statistical mixture

$$\overline{\rho} = \frac{1}{\Delta\phi}\int_{\phi_0 - \frac{\Delta\phi}{2}}^{\phi_0 + \frac{\Delta\phi}{2}} d\phi |\Psi_{OUT}(\phi)\rangle\langle\Psi_{OUT}(\phi)|, \qquad (8)$$

obtained from the average over a number of density matrices $|\Psi_{OUT}(\phi)\rangle\langle\Psi_{OUT}(\phi)|$ each one corresponding to a specific delay phase ϕ. By substituting Eq. (5) in (8) and after a straightforward calculation, we find that $\overline{\rho}$ takes the form:

$$\overline{\rho} = \frac{1}{2}\begin{pmatrix} 1 - \frac{\sin \Delta\phi/2}{\Delta\phi/2}\cos\phi_0 & \frac{\sin \Delta\phi/2}{\Delta\phi/2}\sin\phi_0 \\ \frac{\sin \Delta\phi/2}{\Delta\phi/2}\sin\phi_0 & 1 + \frac{\sin \Delta\phi/2}{\Delta\phi/2}\cos\phi_0 \end{pmatrix}. \quad (9)$$

The diagonal elements of $\overline{\rho}$ describe the probability of finding one electron at the output drains D_0 and D_1, that, in turn, correspond to the signal intensity revealed at the detectors. Such an intensity depends upon both the delay phase ϕ_0 and the noise parameter $\Delta\phi$, as shown in Fig. 2. Once $\overline{\rho}$ has been obtained, the visibility of the

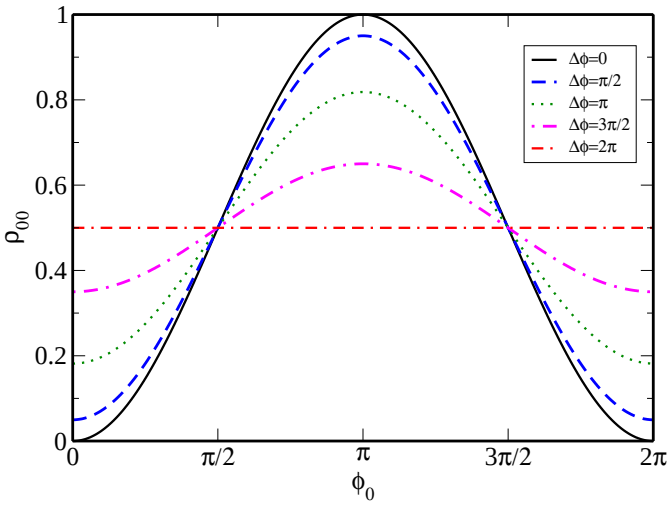

Fig. 2. Single-particle probability of finding the electron of the MZI in the drain D_0 as a function of the phase ϕ_0 for different values of $\Delta\phi$, ranging from 0, no decoherence, to 2π, maximum decoherence.

single-electron can be evaluated. Its expression reads:

$$\nu = \frac{\sin \Delta\phi/2}{\Delta\phi/2}, \quad (10)$$

that is a decreasing function of $\Delta\phi$ in the interval $[0, 2\pi]$. When no noise is considered, namely $\Delta\phi$=0, the results of the previous subsection are found, that is, ρ reduces to $|\Psi_{OUT}(\phi_0)\rangle\langle\Psi_{OUT}(\phi_0)|$ and ν=1. By increasing $\Delta\phi$, the effects of the environmental noise become stronger and the visibility of single-particle interference patterns decreases, as shown in Fig. 2. When $\Delta\phi$=2π, the off-diagonal elements of $\overline{\rho}$ vanish while the diagonal ones tend to 1/2, and ν goes to zero. In this case, the noise destroys completely the quantum interference between the components of the output single-particle wavepackets.

These results suggest that a relation between local single-particle quantities ascribed to wave-particle duality and bipartite non-local properties (loss of coherence) must hold in the system under investigation, in agreement with the well-known complementarity relation introduced for pure two- and multi-qubit states [28,29,30]. In the case of mixed single-particle states, such relation becomes

$$P^2 + \nu^2 + C_G^2 = 1, \quad (11)$$

where P indicates the predictability of the system: in our case a measure of the *a priori* knowledge of whether the electron in the interferometer is in the state $|0\rangle$ or $|1\rangle$. While the visibility ν is related to the wavelike nature of the system, P quantifies the particle-like behavior. C_G is the generalized concurrence which provides a measure of the decoherence undergone by the electron as a consequence of its coupling with the environment, and it is given by $C_G = \sqrt{2(1 - \mathrm{Tr}\overline{\rho}^2)}$.

Let us verify that the relation (11) is satisfied in the setup under investigation. In analogy with the approach

used in Ref. [33], the predictability can be evaluated as $P=|\langle\Theta|\sigma_z|\Theta\rangle|$, where $\sigma_z=\begin{pmatrix}1 & 0\\ 0 & -1\end{pmatrix}$ and $|\Theta\rangle=\frac{|0\rangle+i|1\rangle}{\sqrt{2}}$ is the state describing the electron after crossing the first beam splitter. Our evaluation yields $P=0$. On the other hand, the generalized concurrence results to be

$$C_G = \sqrt{1-\left(\frac{\sin\Delta\phi/2}{\Delta\phi/2}\right)^2}. \qquad (12)$$

By taking into account Eq. (10), the complementarity relation (11) holds for the single-electron mixed state of our setup, as expected. This implies that the loss of coherence of the system can be estimated by means of the single-particle detector response.

3 Two-particle interferometer with no noise

In this section, we first describe a two-electron interferometer given by the Coulomb coupling of two single-electron MZIs. Then, we focus on the close relation between interference effects and two-particle entanglement in absence of environmental noise.

A diagram of the two-electron MZI (2EMZI) is displayed in Fig. 3. Two charge carriers are emitted by the sources S_A and S_B into two single-particle interferometers, namely A and B. Beyond the one-qubit gates, the system involves a conditional phase gate consisting of a coupling block which correlates, via Coulomb interaction, the qubit states of the electrons propagating in the subsystems A and B. Coulomb interaction between electrons has already been proposed as mechanism to entangle waveguide-based qubits and therefore to implement a two-qubit gate [17, 11, 10].

The coupling block sketched in Fig. 3 consists of a section of length l where the inner waveguides, namely 1_A and 0_B, are brought close to each other in order to "activate" the Coulomb repulsion between the electrons travelling in those channels. Without loss of generality,

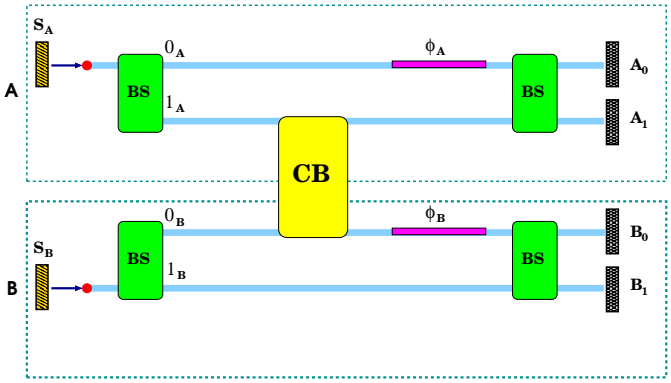

Fig. 3. Sketch of the electron waveguide network used to implement the 2EMZI. The two electrons are injected from the sources S_A and S_B, and each one propagates in one couple of channels, i.e. a single MZI, involving two beam splitters and a delaying barrier potential inducing a change of phase of ϕ_A, and ϕ_B for the upper and lower interferometer, respectively. In case no decoherence effects are considered, the phase $\phi_{A(B)}$ accumulated along channel 0 of the $A(B)$ MZI is a deterministic variable. Otherwise, it is a stochastic variable described by a flat distribution. The coupling block (CB) correlates the qubit states of the two single-particle MZI's by means of the Coulomb interaction between the electron wavefunctions propagating along the inner channels. Finally, the carrier injected by the source S_A (S_B) is collected by the drains $\{A_0, A_1\}$ ($\{B_0, B_1\}$).

we adopt a model of Coulomb gate already introduced in Ref. [10]. The Coulomb energy potential between the

two particles in the inner channels has been taken proportional to the inverse of the distance D within the interaction window, i.e. $V_{CO} = e^2/(4\pi\epsilon D)$, and zero elsewhere. In such a scheme, each of the two particles crossing the coupling block feels a rectangular barrier potential V_{CO} high and l wide. Thus the phase change γ in the network state $|0_B 1_A\rangle$ related to electron travelling through the interaction window can be analytically evaluated by means of the time-independent approach already used in the Sec. 2 to analyze the electron phase shifter. Within the approximation of electron energies much larger than V_{CO} in order to prevent reflections, the transmission probability results about 1, while the phase change is given by $\gamma = -\sqrt{\frac{2m}{E}}\frac{e^2}{8\pi\hbar\epsilon D}$ and, as expected, depends both upon the physical parameters of the carriers and the geometry of the coupling block. In turn, these affect the amount of quantum correlations created between the two particles. In the following, we will consider values of γ ranging from 0 to 2π.

The matrix representation of the conditional phase gate discussed above in the two-qubit base $\{|0_A 0_B\rangle, |0_A 1_B\rangle, |1_A 0_B\rangle, |1_A 1_B\rangle\}$ is

$$T(\gamma) = \begin{pmatrix} 1 & 0 & 0 & 0 \\ 0 & 1 & 0 & 0 \\ 0 & 0 & e^{i\gamma} & 0 \\ 0 & 0 & 0 & 1 \end{pmatrix}. \qquad (13)$$

Once crossed the coupling block, the electrons propagating in the 1D waveguides interact with the two potential barriers placed in the 0_A and 0_B channels, inducing a phase change of ϕ_A and ϕ_B, respectively. Then, the particles interfere again and finally are collected by the detectors at the output drains $\{A_0, A_1, B_0, B_1\}$. Thus, the global logical transformation on the two-particle input state $|\Phi_{IN}\rangle$=$|0_A 1_B\rangle$ can be written as:

$$R_y^A\left(\frac{\pi}{2}\right) R_y^B\left(\frac{\pi}{2}\right) R_0^B(\phi_B) R_0^A(\phi_A) T^{AB}(\gamma) R_y^A\left(\frac{\pi}{2}\right) R_y^B\left(\frac{\pi}{2}\right), \qquad (14)$$

where the superscripts of the quantum gates indicate which subsystem they act on. After a straightforward calculation, we find that the output state $|\Phi_{OUT}\rangle$ takes the form

$$\begin{aligned} |\Phi_{OUT}\rangle = \sum_{X,Y=0}^{1} \alpha_{XY}(\gamma)|X_A Y_B\rangle = \frac{1}{2} e^{i\left(\frac{\phi_B}{2}+\phi_A\right)} \times \qquad (15) \\ \Bigg[i\left(\cos\frac{\phi_B}{2} - e^{i\left(\frac{\gamma}{2}-\phi_A\right)}\cos\frac{\phi_B+\gamma}{2}\right)|0_A 0_B\rangle \\ + i\left(e^{i\left(\frac{\gamma}{2}-\phi_A\right)}\sin\frac{\phi_B+\gamma}{2} - \sin\frac{\phi_B}{2}\right)|0_A 1_B\rangle \\ - \left(\cos\frac{\phi_B}{2} + e^{i\left(\frac{\gamma}{2}-\phi_A\right)}\cos\frac{\phi_B+\gamma}{2}\right)|1_A 0_B\rangle \\ + \left(e^{i\left(\frac{\gamma}{2}-\phi_A\right)}\sin\frac{\phi_B+\gamma}{2} + \sin\frac{\phi_B}{2}\right)|1_A 1_B\rangle \Bigg]. \end{aligned}$$

Such an expression describes the two electrons at the output drains in a non-separable state where the amount of quantum correlations between the qubits depends upon the phase γ.

3.1 Entanglement

Here the carrier-carrier entanglement is evaluated in terms of the Wotters concurrence [40] obtained from the two-particle density matrix ρ^{AB} as

$$C = \max\{0, \sqrt{\lambda_1} - \sqrt{\lambda_2} - \sqrt{\lambda_3} - \sqrt{\lambda_4}\}, \qquad (16)$$

where λ_i are the eigenvalues of the matrix ζ

$$\zeta = \sqrt{\rho^{AB}}(\sigma_y^A \otimes \sigma_y^B)\rho^{AB*}(\sigma_y^A \otimes \sigma_y^B)\sqrt{\rho^{AB}} \qquad (17)$$

arranged in decreasing order. Here, ρ^{AB*} denotes the complex conjugation of ρ^{AB} in the standard basis, and $\sigma_y^{A(B)}$ is the well-known Pauli matrix acting on the qubit state of the subsystem $A(B)$. C ranges from 0, for a disentangled state, to 1, for a maximally correlated state. For a pure two-qubit state, the concurrence corresponds to the generalized concurrence C_G defined in the previous section. Indeed, the qubit-qubit entanglement can also be interpreted as the loss of decoherence undergone by a qubit as a consequence of its interaction with the other qubit considered as the environment.

For the output state $\rho^{AB} = |\Phi_{OUT}\rangle\langle\Phi_{OUT}|$ describing the electrons at the drains, C is given by

$$C = \sin\frac{\gamma}{2}. \tag{18}$$

When $\gamma = 0$, the output state, does not exhibit quantum correlations. On the other hand, for $\gamma{=}\pi$ a maximally entangled state is obtained. As a matter of fact, if now the two electrons at drains are processed by the network of one-qubit gates

$$R_y^B\left(\frac{\pi}{2}\right) R_0^B(-\phi_B) R_0^A(-\phi_A) R_y^B\left(-\frac{\pi}{2}\right) R_y^A\left(-\frac{\pi}{2}\right)$$

the Bell state $i/\sqrt{2}\,(|0_A 0_B\rangle + |1_A 1_B\rangle)$ is produced.

3.2 Interference

Let us focus our attention on the single-particle quantum interference described by Eq. (15). To this aim, we need to estimate the one-particle reduced density matrices $\rho^{A(B)}{=}\mathrm{Tr}_{B(A)}\rho^{AB}$. After straightforward calculations, we find:

$$\rho^A = \frac{1}{2}\begin{pmatrix} 1 - F(\phi_A,-\gamma) & G(\phi_A,-\gamma) \\ G(\phi_A,-\gamma) & 1 + F(\phi_A,-\gamma) \end{pmatrix}, \tag{19}$$

and

$$\rho^B = \frac{1}{2}\begin{pmatrix} 1 + F(\phi_B,\gamma) & -G(\phi_B,\gamma) \\ -G(\phi_B,\gamma) & 1 - F(\phi_B,\gamma) \end{pmatrix}, \tag{20}$$

where

$$\begin{aligned} F(\phi,\gamma) &= \frac{1}{2}\left[\cos\phi + \cos(\phi+\gamma)\right], \\ G(\phi,\gamma) &= \frac{1}{2}\left[\sin\phi + \sin(\phi+\gamma)\right]. \end{aligned} \tag{21}$$

For both interferometers, the visibility of the single-particle interference fringes is given by

$$\nu_{A(B)} = \left|\cos\frac{\gamma}{2}\right|. \tag{22}$$

When no qubit-qubit entanglement is created, namely $\gamma{=}0$, the two interferometers are completely uncorrelated and the electron detection probabilities are described by sinusoidal functions $\sin^2\frac{\phi_{A(B)}}{2}$ and $\cos^2\frac{\phi_{A(B)}}{2}$ of the local phase $\phi_{A(B)}$. In this case, the visibility takes its maximal value 1. The more correlated are the particles (i.e. the greater is the loss of coherence undergone by an electron as a consequence of the electron-electron interaction) the smaller is the visibility of single-electron interference. When entanglement reaches its maximum value, quantum interference between the components of the output single-particle wavepackets is completely destroyed. This is in agreement with the results of Sec. 2 for the single-electron MZI subject to environmental noise.

In agreement with the theoretical predictions [31,32], the complementarity relation

$$C^2 + \nu_{A(B)}^2 + P_{A(B)}^2 = 1, \tag{23}$$

holds in the 2EMZI. The predictability $P_{A(B)}=\left|\langle\Xi|\sigma_z^{A(B)}|\Xi\rangle\right|$ values, two-particle fringes become more and more visible ($|\Xi\rangle$ describes the two electrons after the coupling block) is zero like the case of single-electron MZI. Therefore, here the qubit-qubit entanglement can simply be related to the single-particle visibility as $C=\sqrt{1-\nu^2}$. The expression gives a useful tool to quantify the amount of quantum correlations and therefore the measure of the loss of single-particle coherence due to electron-electron interaction. Such a measurement relies on single-particle detectors response in an experimental setup of 2EMZI where decoherence effects are negligible.

A complementary relation of the type given in Eq. (23) can also be established between one-particle and two-particle interference, as argued by Jager *et al.* [28,29]. Two-particle effects are related to the joint probability of detecting one electron at A_X and the other one at B_Y in a measure performed by detectors at the output drains. However, such a detection probability, given by the square modulus of the coefficient α_{XY}, can exhibit non *genuine* two-particle interference related to the single-particle probabilities of finding the electron of the interferometer A in the channel A_X and the other electron in the channel B_Y. In order to evaluate *genuine* two-particle effects, some authors [28, 29] proposed to use a "corrected" joint two-particle probability P_{XY} given by

$$P_{XY} = |\alpha_{XY}|^2 - \rho^A_{XX}\rho^B_{YY} + \frac{1}{4}. \qquad (24)$$

In Fig. 4 we have reported P_{00} as a function of the phases ϕ_A and ϕ_B. While for zero entanglement, such a probability assumes the constant value 1/4 for all the phases as the degree of entanglement increases. In fact, P_{00} can

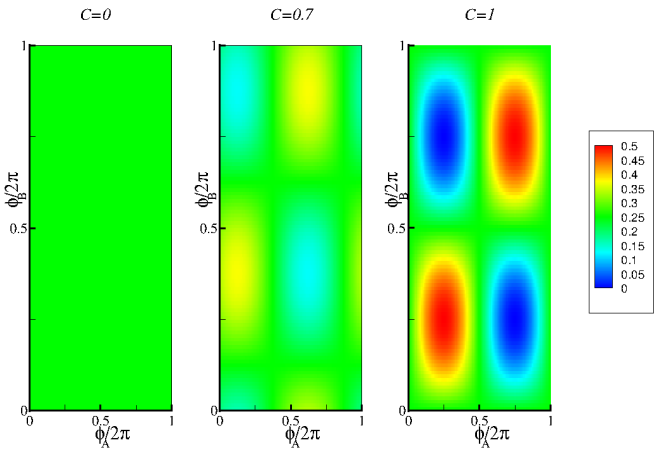

Fig. 4. The "corrected" joint probability P_{00} of finding two electrons at drains A_0 and B_0 as a function of ϕ_A and ϕ_B for three different values of C, namely 0, 0.7, and 1. The visibility of two-particle fringes increases with C. Note that the tailoring of C affects not only the magnitude of P_{00} but also its dependence on the two phases.

be used to quantify the two-particle visibility ν_{12}:

$$\nu_{12} = \frac{[P_{00}]\text{max} - [P_{00}]\text{min}}{[P_{00}]\text{max} + [P_{00}]\text{min}} = \sin^2\frac{\gamma}{2} = C^2, \qquad (25)$$

which results to be the square of the concurrence, in agreement with the results presented in the literature showing the close relation between entanglement and two-particle visibility [31]. As expected, the two-particle visibility is zero for γ=0, i.e. the two-particle interference effects are due only to single-particle fringes. On the other hand, ν_{12} reaches the maximum value for $\gamma=\pi$, when the electron-electron correlation gives rise to genuine two-particle fringes. In agreement with the well-known complementarity inequality [28,29], an increase of ν_{12} corresponds to a de-

crease of the visibility of the one-particle fringes, and vice versa:

$$\nu_{A(B)}^2 + \nu_{12}^2 = \cos^2\frac{\gamma}{2} + \sin^4\frac{\gamma}{2} \leq 1. \tag{26}$$

ν_{12} could be also used, at least in principle, to quantify the degree of the qubit-qubit entanglement. Nevertheless, in an experimental implementation of our setup the estimation of the visibility of two-particle interference would certainly be more complex than the one of ν, since it requires the simultaneous detection of two electrons in two different detectors.

4 Effects of noise on a two-particle interferometer

Here, we analyze how the environmental noise affects the interference and entanglement of the setup sketched in Fig. 3.

In agreement with the approach used in Sec. 2, the noise is assumed to randomize the phases ϕ_A and ϕ_B of the two carriers. Such dephasing effects are independent of each other since the fluctuations of the potential barriers of the channels 0 of the two MZIs are assumed to be due to different noise sources. $\phi_{A(B)}$ is described by the flat distribution $P(\phi_{A(B)})$ of Eq. (7) with parameters $\phi_{0\,A(B)}$ and $\Delta\phi_{A(B)}$. The two particles arriving at the drains $\{A_0, A_1, B_0, B_1\}$ will be in the mixed state

$$\overline{\rho^{AB}} = \frac{1}{\Delta\phi_A\Delta\phi_B}\int_{\phi_{0\,A}-\frac{\Delta\phi_A}{2}}^{\phi_{0\,A}+\frac{\Delta\phi_A}{2}} d\phi_A \times \int_{\phi_{0\,B}-\frac{\Delta\phi_B}{2}}^{\phi_{0\,B}+\frac{\Delta\phi_B}{2}} d\phi_B |\Phi_{OUT}(\phi_A,\phi_B)\rangle\langle\Phi_{OUT}(\phi_A,\phi_B)|. \tag{27}$$

Its explicit evaluation is given in Appendix A. For the sake of simplicity, we will assume that the spectra of the environmental noises on the two MZIs, namely their dephasing, are identical even if they stem from different sources. Such an assumption means that $\Delta\phi_A{=}\Delta\phi_B{=}\Delta\phi$.

4.1 Entanglement

First, we estimate the qubit-qubit entanglement in terms of concurrence defined in the previous section. By inserting Eqs. (37) in Eq. (17), we can compute the concurrence for the mixed state of Eq. (27)

$$\overline{C} = \max\{0, g\}, \tag{28}$$

where

$$g = \frac{\sin\Delta\phi/2}{\Delta\phi/2}\sin\frac{\gamma}{2} - \frac{1}{2}\left[1 - \left(\frac{\sin\Delta\phi/2}{\Delta\phi/2}\right)^2\right]. \tag{29}$$

In Fig. 5, we have reported $\overline{C}$ as a function of γ for different values of $\Delta\phi$. As expected, for zero dephasing the concurrence exhibits a sinusoidal dependence against the phase γ. This allows us to quantify the qubit-qubit entanglement and to expose its reduction with the noise. Indeed, in this case expression (29) reduces to Eq. (18) obtained for the 2EMZI in absence of noise. When noise effects are taken into account, the entanglement exhibits a peculiar behavior. Not only the maximum amount of quantum correlations created between two qubits decreases as $\Delta\phi$ increases, but $\overline{C}$ vanishes even when the Coulomb coupling between the two MZIs is different from zero. Specifically, the $\Delta\gamma$ phase interval over which electron-electron entanglement takes non zero values is related to $\Delta\phi$ by the

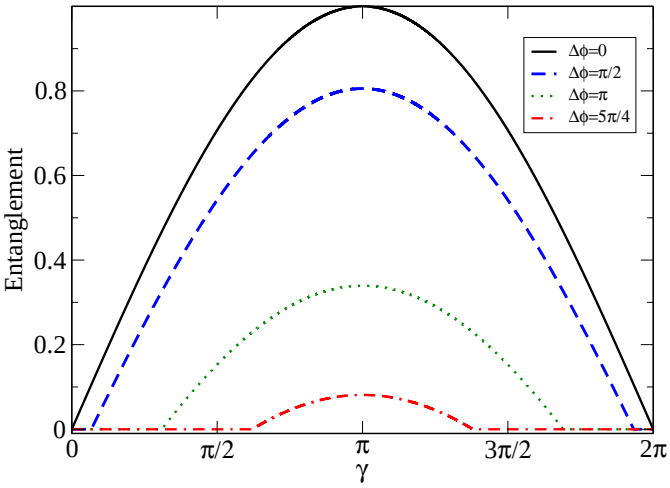

Fig. 5. Electron-electron entanglement as a function of the Coulomb-induced phase γ evaluated for different values of $\Delta\phi$ indicated in the legend. Note that for $\Delta\phi \geq \Delta\phi_c \approx 1.33\pi$ entanglement is identically zero for any value of γ.

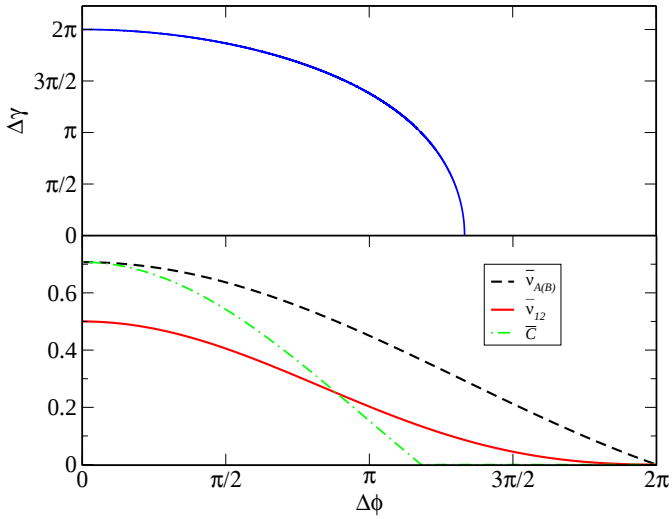

Fig. 6. Top panel: The interval $\Delta\gamma$ over which entanglement takes non zero values as a function of $\Delta\phi$. Bottom panel: single-particle visibility $\overline{\nu}_{A(B)}$ (dashed line), two-particle visibility $\overline{\nu}_{12}$ (solid line), and entanglement $\overline{C}$ (dash-dotted line) as a function of $\Delta\phi$ with γ=$\pi/2$.

expression

$$\Delta\gamma = 2\pi - 4\arcsin\left(\frac{1-\left(\frac{\sin\Delta\phi/2}{\Delta\phi/2}\right)^2}{\frac{2\sin\Delta\phi/2}{\Delta\phi/2}}\right). \qquad (30)$$

As shown in the top panel of Fig. 6, $\Delta\gamma$ decreases rapidly with noise intensity and goes to zero when the carrier dephasing induced by the environment reaches the critical value $\Delta\phi_c \approx 1.33\pi$, where the latter value is obtained from the relation $\frac{\sin\Delta\phi_c/2}{\Delta\phi_c/2}$=$\sqrt{2}-1$. When $\Delta\phi = \Delta\phi_c$, the degree of entanglement is identically zero for any value of γ. In other terms, in our setup there is no need to reach the maximum dephasing effects in order to inhibit completely the entanglement production. These results clearly indicate that the randomization of the phase carrier is very effective into destroying the quantum correlation created between the two carriers as a consequence of their mutual repulsion. In this view, the entangled states produced in our device thanks to Coulomb coupling are not very robust under decoherence phenomena.

4.2 Interference

Now, we examine the effects of noise on the visibility of the fringes of one- and two-particle interference in the 2EMZI. Following the approach adopted in the previous section, the former can be evaluated from the single-particle reduced density matrix $\overline{\rho^{A(B)}}$ describing the electron of subsystem $A(B)$. This can simply be expressed in terms of $\rho^{A(B)}$ as

$$\overline{\rho^{A(B)}}_{ij} = \frac{\sin\Delta\phi/2}{\Delta\phi/2}\rho_{ij}^{A(B)} + \delta_{ij}\frac{1}{2}\left(1-\frac{\sin\Delta\phi/2}{\Delta\phi/2}\right), \quad (31)$$

where δ_{ij} is the Kronecker delta. After a straightforward calculation, we get the visibility of the one-particle inter-

ference:

$$\overline{\nu}_{A(B)} = \nu_{A(B)} \frac{\sin \Delta\phi/2}{\Delta\phi/2} = \left|\cos \frac{\gamma}{2}\right| \frac{\sin \Delta\phi/2}{\Delta\phi/2}. \qquad (32)$$

$\overline{\nu}_{A(B)}$ is given by the product of the visibility $\nu_{A(B)}$, found for the system in absence of noise (see Eq. (22)) and related to the Coulomb interaction by means of the phase γ, and of the factor $\frac{\sin \Delta\phi/2}{\Delta\phi/2}$, which represents the visibility of a MZI, not coupled to other systems in the presence of environmental noise inducing phase randomization of the carriers, as shown in Eq. (10). Eq. (32) is in agreement with the fact that, for the setup under investigation, the two decoherence channels of the single-electron wavefunctions, one due to electron-electron interaction and the other one due to the environmental noise, are uncorrelated. Therefore, the effects of these two mechanisms on the single-electron visibility are independent of each other.

By suitably revising Eq. (11), the complementarity relation between single-particle and non-local quantities is still satisfied. As stated above, now two independent decoherence channels are active and therefore the qubit-qubit entanglement alone cannot be used to quantify the decoherence undergone by a single qubit. The latter has to be evaluated in terms of the generalized concurrence $\overline{C_G}$, defined in Sec. 2, which allows one to estimate the total loss of coherence of the single-electron wavefunctions. For the 2EMZI subject to the environmental noise $\overline{C_G}^{A(B)}$ takes the form

$$\overline{C_G}^{A(B)} = \sqrt{1 - \left(\frac{\sin \Delta\phi/2}{\Delta\phi/2}\right)^2 \cos^2 \frac{\gamma}{2}}. \qquad (33)$$

In comparison with the behavior exhibited by the two-electron entanglement, we note that for a given value of γ the one-particle decoherence is maximum (C_G=1) only when noise effects are maximum ($\Delta\phi = 2\pi$). By taking into account that predictability vanishes, Eqs. (32) and (33) imply that the complementarity relation between visibility and loss of single-particle coherence still holds for the mixed state produced in our 2EMZI.

Finally, we investigate the two-particle interference. In order to discriminate *genuine* two-electron effects from the ones deriving from single-particle detection probabilities when the noise effects are present, we use a suitable revised form of Eq. (24):

$$\overline{P}_{XY} = \overline{\rho^{AB}}_{XYXY} - \overline{\rho^{A}_{XX}} \quad \overline{\rho^{B}_{YY}} + \frac{1}{4}, \qquad (34)$$

where $\overline{\rho^{AB}}_{XYXY}$ has been introduced to describe the joint probability of detecting one electron at drain A_X and the other one at B_Y. As expected, the *genuine* two-particle interference effects, described by $\overline{P}_{XY}$, are affected by noise. Two-particle fringes are less visible for higher disorder, as clearly indicated by the two-particle visibility

$$\overline{\nu}_{12} = \left(\frac{\sin \Delta\phi/2}{\Delta\phi/2}\right)^2 \sin^2 \frac{\gamma}{2} \qquad (35)$$

which goes to zero for $\Delta\phi$=2π. The complementarity inequality relating $\overline{\nu}$ to $\overline{\nu}_{12}$ is still valid:

$$\overline{\nu}^2_{A(B)} + \overline{\nu}^2_{12} = \left(\frac{\sin \Delta\phi/2}{\Delta\phi/2}\right)^2 \cos^2 \frac{\gamma}{2} + \left(\frac{\sin \Delta\phi/2}{\Delta\phi/2}\right)^4 \sin^4 \frac{\gamma}{2} \leq 1. \qquad (36)$$

Unlike the results found in Sec. 3, here $\overline{\nu}_{12}$ cannot be used as an estimator of electron-electron entanglement. Indeed, two-particle interference can be detected at the output drains even if the degree of quantum correlation between the carriers is zero as indicated in the bottom

panel of Fig. 6. Nevertheless, we stress that in an experimental implementation of our setup the entanglement can still be estimated, at least in principle, by means of single-particle and two-particle detector responses. As shown in Eq. (29), entanglement depends only upon the two independent parameters γ and $\Delta\phi$ which appear in the expressions (32) and (35) describing visibility of one- and two-particle interference, respectively. An estimate of $\overline{\nu}$ and $\overline{\nu}_{12}$ permits to evaluate γ and $\Delta\phi$, and, in turn, the entanglement.

5 Conclusions

Beyond its specific role in the experimental validation of quantum mechanics, electron transport in 1D waveguides constitues an important resource both for the realization of electronic interferometers [6,8,9] and for the design of next-generation electron devices capable of processing quantum information [17,18,19]. The main threat to these implementations is represented by dephasing mechanisms which strongly affect the coherence of the quantum systems.

In this work, we have analytically investigated the interference phenomena and the appearance of non-local effects in one- and two-electron interferometers realized by means of 1D channels and subject to an environmental noise. The latter stems from the fluctuations of the confining potential of the interferometer arms and leads to a random detune of the transmission phase of the carriers. As shown in the literature [41,42], nanometric few-electron systems are very sensitive to the random nature of intrinsic impurities and to the effects of quasi-static fluctuation of background charge. Our model treats such noise classically by neglecting the building up of quantum entanglement between the above background and our system, namely the charge carriers along the waveguides. Furthermore, a single noise source is included in our calculations. This has to be considered as a first step towards the fully quantitative modeling of a real device whose functioning relies on the coherence of the quantum system, with the inclusion of all the relevant sources of noise as, for example, amplifier noise, gate noise or elastic phonon scattering.

In order to validate our approach, first we have studied the dephasing in an electronic version of a single-particle MZI, using only single-qubit logical operations. We have found that the single-electron visibility is related to the loss of coherence induced by the environmental noise. Indeed, the greater are the noise effects, the smaller is the visibility of the single-electron interference fringes. In the noisy MZI, the well-know complementarity relation [28, 29] linking single-particle quantities to non-local quantities, such as the loss of coherence, is thus satisfied. This proves the feasibility of our procedure to evaluate the features of dephasing in electron interference and entanglement in 1D channels.

In the second part of the paper, we have examined the two-electron interferometer given by the coupling of two single-electron MZIs through the Coulomb interaction. The latter was shown to yield quantum correlations between the carriers in other systems realized with 1D electron waveguides [17]. In the absence of environmen-

tal noise, complementarity is found between the visibility of single-electron interference fringes and electron-electron entanglement, which also represents an estimate of the loss of quantum coherence of an electron due to its interaction with the other carriers. Quantum correlations stemming from the Coulomb interaction between electrons affect also the visibility of the *genuine* two-particle interference fringes, ax explained in Sec. 3.2. The latter turns out to increase with the square of the entanglement. These results suggest that the response of single-and two-particle detectors at the output drains could give a quantitative estimation of the electron-electron entanglement in an experimental implementation of our system.

Finally, dephasing mechanisms have been introduced in the two-electron interferometer. We have found that the entangled states, obtained thanks to the electron-electron interaction, are not very robust with respect to decoherence. Indeed, also for the case of optimal tuning of the geometrical parameters of the setup (leading to maximum entanglement in absence of noise) quantum correlations between the carriers can be completely destroyed by the environmental noise, even when the latter does not yield maximum dephasing, thus partially preserving single-electron interference. This is a remarkable result, since it shows analytically that a small amount of noise not only reduces entanglement but it completely suppresses quantum correlations unless the coupling between the two subsystems is strong enough.

The visibility of the pattern of the single-particle interference results to be degraded by decoherence due both to the mutual repulsion between the two carriers and to environmental noise effects. In particular, our results indicate that these mechanisms act as two independent and separate decoherence channels for one-electron states. As a consequence, the one-particle visibility is not linked by a complementarity relation to electron-electron entanglement but to the total loss of coherence. Noise plays also a key role in the analysis of *genuine* two-particle interference fringes. Their visibility, degrading with the intensity of the noise, is somehow related to the one-electron visibility by a suitable generalization of the complementarity inequality holding for pure two-qubit states [28,29]. Unlike what was found in absence of noise, the two-particle visibility cannot be taken as an evaluator of the entanglement. Nevertheless, in an experimental realization of the two-electron interferometer, the estimate of the one- and two-particle visibility can be obtained by means of the single- and cross-correlated detection of the carriers in two drains, respectively. Then, it can be used to evaluate the noise and Coulomb coupling parameters and, from these, both entanglement and decoherence. This shows that 1D channel architectures are a powerful means to investigate entanglement and dephasing in electron interference.

A Two-particle density matrix of the noisy two-electron interferometer

Here we report the elements of the average density matrix describing two electrons arriving at the output drains in the noisy two-particle interferometer exploting Coulomb

interaction. The double integrals in the r.h.s of Eq. (27)

yield

$$\overline{\rho^{AB}}_{0000} = \frac{1}{4}\left[1+\frac{1}{2}f_B\Big(\cos\phi_{B0}+\cos\left(\phi_{B0}+\gamma\right)\Big)-f_A\cos\Big(\phi_{A0}-\frac{\gamma}{2}\Big)\Big(\cos\frac{\gamma}{2}+f_B\cos\Big(\phi_{B0}+\frac{\gamma}{2}\Big)\Big)\right]$$

$$\overline{\rho^{AB}}_{0101} = \frac{1}{4}\left[1-\frac{1}{2}f_B\Big(\cos\phi_{B0}+\cos\left(\phi_{B0}+\gamma\right)\Big)-f_A\cos\Big(\phi_{A0}-\frac{\gamma}{2}\Big)\Big(\cos\frac{\gamma}{2}-f_B\cos\Big(\phi_{B0}+\frac{\gamma}{2}\Big)\Big)\right]$$

$$\overline{\rho^{AB}}_{1010} = \frac{1}{4}\left[1+\frac{1}{2}f_B\Big(\cos\phi_{B0}+\cos\left(\phi_{B0}+\gamma\right)\Big)+f_A\cos\Big(\phi_{A0}-\frac{\gamma}{2}\Big)\Big(\cos\frac{\gamma}{2}+f_B\cos\Big(\phi_{B0}+\frac{\gamma}{2}\Big)\Big)\right]$$

$$\overline{\rho^{AB}}_{1111} = \frac{1}{4}\left[1-\frac{1}{2}f_B\Big(\cos\phi_{B0}+\cos\left(\phi_{B0}+\gamma\right)\Big)+f_A\cos\Big(\phi_{A0}-\frac{\gamma}{2}\Big)\Big(\cos\frac{\gamma}{2}-f_B\cos\Big(\phi_{B0}+\frac{\gamma}{2}\Big)\Big)\right]$$

$$\begin{aligned}\overline{\rho^{AB}}_{0001} = \frac{1}{4}\Big\{ & f_B\left[f_A\cos\Big(\phi_{A0}-\frac{\gamma}{2}\Big)\sin\Big(\phi_{B0}+\frac{\gamma}{2}\Big)-\frac{1}{2}\Big(\sin\phi_{B0}+\sin\left(\phi_{B0}+\gamma\right)\Big)\right]+\\ & +if_A\sin\frac{\gamma}{2}\sin\Big(\phi_{A0}-\frac{\gamma}{2}\Big)\Big\}\end{aligned}$$

$$\begin{aligned}\overline{\rho^{AB}}_{0010} = \frac{1}{4}\Big\{ & f_B\left[f_A\sin\Big(\phi_{A0}-\frac{\gamma}{2}\Big)\cos\Big(\phi_{B0}+\frac{\gamma}{2}\Big)+\frac{i}{2}\Big(\cos\left(\phi_{B0}+\gamma\right)-\cos\phi_{B0}\Big)\right]+\\ & +f_A\cos\frac{\gamma}{2}\sin\Big(\phi_{A0}-\frac{\gamma}{2}\Big)\Big\}\end{aligned}$$

$$\begin{aligned}\overline{\rho^{AB}}_{0011} = \frac{1}{4}\Big\{ & -f_B\left[f_A\sin\Big(\phi_{A0}-\frac{\gamma}{2}\Big)\sin\Big(\phi_{B0}+\frac{\gamma}{2}\Big)+\frac{i}{2}\Big(\sin\left(\phi_{B0}+\gamma\right)-\sin\phi_{B0}\Big)\right]+\\ & +if_A\sin\frac{\gamma}{2}\cos\Big(\phi_{A0}-\frac{\gamma}{2}\Big)\Big\}\end{aligned}$$

$$\begin{aligned}\overline{\rho^{AB}}_{0110} = \frac{1}{4}\Big\{ & -f_B\left[f_A\sin\Big(\phi_{A0}-\frac{\gamma}{2}\Big)\sin\Big(\phi_{B0}+\frac{\gamma}{2}\Big)+\frac{i}{2}\Big(\sin\left(\phi_{B0}+\gamma\right)-\sin\phi_{B0}\Big)\right]+\\ & -if_A\sin\frac{\gamma}{2}\cos\Big(\phi_{A0}-\frac{\gamma}{2}\Big)\Big\}\end{aligned}$$

$$\begin{aligned}\overline{\rho^{AB}}_{0111} = \frac{1}{4}\Big\{ & -f_B\left[f_A\sin\Big(\phi_{A0}-\frac{\gamma}{2}\Big)\cos\Big(\phi_{B0}+\frac{\gamma}{2}\Big)+\frac{i}{2}\Big(\cos\left(\phi_{B0}+\gamma\right)-\cos\phi_{B0}\Big)\right]+\\ & +f_A\cos\frac{\gamma}{2}\sin\Big(\phi_{A0}-\frac{\gamma}{2}\Big)\Big\}\end{aligned}$$

$$\begin{aligned}\overline{\rho^{AB}}_{1011} = \frac{1}{4}\Big\{ & -f_B\left[f_A\cos\Big(\phi_{A0}-\frac{\gamma}{2}\Big)\sin\Big(\phi_{B0}+\frac{\gamma}{2}\Big)+\frac{1}{2}\Big(\sin\phi_{B0}+\sin\left(\phi_{B0}+\gamma\right)\Big)\right]+\\ & -if_A\sin\frac{\gamma}{2}\sin\Big(\phi_{A0}-\frac{\gamma}{2}\Big)\Big\},\end{aligned} \tag{37}$$

where $f_{A(B)}=\frac{\sin \Delta\phi_{A(B)}/2}{\Delta\phi_{A(B)}/2}$ is the visibility of the single-particle interference of the subsystem $A(B)$ when the two MZIs are not coupled.

References

1. H. Grabert, M. Devoret, eds., *Single Charge Tunneling* (Plenum, NY, 1992)
2. Z.A.K. Durrani, *Single-Electron Devices and Circuits in Silicon* (Cambridge University Press, Cambridge, 2009)
3. M.A. Kastner, Rev. Mod. Phys. **64**, 849 (1992)
4. J. Dressel, Y. Choi, A.N. Jordan, Phys. Rev. B **85**, 045320 (2012)
5. F. Buscemi, P. Bordone, A. Bertoni, Journal of Physics: Condensed Matter **21**, 305303 (2009)
6. A.T. Tilke, F.C. Simmel, H. Lorenz, R.H. Blick, J.P. Kotthaus, Phys. Rev. B **68**, 075311 (2003)
7. M. Yamamoto, S. Takada, C. Baeuerle, K. Watanabe, A.D. Wieck, S. Tarucha, Nature Nanotechnology **7**, 247 (2012)
8. Y. Ji, Y. Chung, D. Sprinzak, M. Heiblum, D. Mahalu, H. Shtrikman, Nature **422**, 415 (2003)
9. I. Neder, N. Ofek, Y. Chung, M. Heiblum, D. Mahalu, V. Umansky, Nature **448**, 333 (2007)
10. G.B. Akguc, L.E. Reichl, A. Shaji, M.G. Snyder, Phys. Rev. A **69**, 042303 (2004)
11. L.E. Reichl, M.G. Snyder, Phys. Rev. A **72**, 032330 (2005)
12. R.Q. Yang, J.M. Xu, Phys. Rev. B **43**, 1699 (1991)
13. C.C. Eugster, J.A. del Alamo, M.J. Rooks, M.R. Melloch, App. Phys. Lett. **64**, 3157 (1994)
14. T. Morimoto *et al.*, App. Phys. Lett. **82**, 3952 (2003)
15. A. Ramamoorthy, J.P. Bird, J.L. Reno, App. Phys. Lett. **89**, 013118 (2006)
16. A. Ramamoorthy, L. Mourokh, J.L. Reno, J.P. Bird, Phys. Rev. B **78**, 035335 (2008)
17. A. Bertoni, P. Bordone, R. Brunetti, C. Jacoboni, S. Reggiani, Phys. Rev. Lett. **84**, 5912 (2000)
18. F. Buscemi, P. Bordone, A. Bertoni, Phys. Rev. B **81**, 045312 (2010)
19. F. Buscemi, Phys. Rev. A **83**, 012302 (2011)
20. D. Giulini *et al.*, *Decoherence and the Appearance of a Classical World in Quantum Theory* (Springer, 1996), ISBN 9783540613947
21. W.H. Zurek, Rev. Mod. Phys. **75**, 715 (2003)
22. A. Stern, Y. Aharonov, Y. Imry, Phys. Rev. A **41**, 3436 (1990)
23. S.A. van Langen, M. Büttiker, Phys. Rev. B **56**, R1680 (1997)
24. J.H. Davies, J.C. Egues, J.W. Wilkins, Phys. Rev. B **52**, 11259 (1995)
25. F. Marquardt, C. Bruder, Phys. Rev. B **70**, 125305 (2004)
26. F. Marquardt, C. Bruder, Phys. Rev. Lett. **92**, 056805 (2004)
27. S.G. Jakobs, V. Meden, H. Schoeller, T. Enss, Phys. Rev. B **75**, 035126 (2007)
28. G. Jaeger, M.A. Horne, A. Shimony, Phys. Rev. A **48**, 1023 (1993)
29. G. Jaeger, A. Shimony, L. Vaidman, Phys. Rev. A **51**, 54 (1995)
30. X. Peng, X. Zhu, D. Suter, J. Du, M. Liu, K. Gao, Phys. Rev. A **72**, 052109 (2005)
31. M. Jakob, J.A. Bergou, Opt. Comm. **283**, 827 (2001)
32. J. Suzuki, C. Miniatura, K. Nemoto, Phys. Rev. A **81**, 062307 (2010)

33. X. Peng, J. Zhang, J. Du, D. Suter, Phys. Rev. A **77**, 052107 (2008)
34. M. Born, E. Wolf, *Principles of Optics* (Cambridge University Press, Cambridge, 1999)
35. T. Zibold, P. Vogl, A. Bertoni, Phys. Rev. B **76**, 195301 (2007)
36. A. Bertoni, P. Bordone, R. Brunetti, C. Jacoboni, S. Reggiani, Journal of Modern Optics **49**, 1219 (2002)
37. V. Corato, P. Silvestrini, A. Görlich, P. Korcyl, J. Wosiek, L. Stodolsky, Phys. Rev. B **75**, 184507 (2007)
38. D. Rossini, G. Benenti, G. Casati, Phys. Rev. E **74**, 036209 (2006)
39. A. Amir, Y. Lahini, H.B. Perets, Phys. Rev. E **79**, 050105 (2009)
40. W.K. Wootters, Phys. Rev. Lett. **80**, 2245 (1998)
41. M. Furlan, S.V. Lotkhov, Phys. Rev. B **67**, 205313 (2003)
42. J. Johansson, D.B. Haviland, Phys. Rev. B **63**, 014201 (2000)